Electronic Supplementary Information

Chemical Synthesis of Stimuli-Responsive Guide RNA for Conditional Control of CRISPR-Cas9 Gene Editing

Chunmei Gu, Lu Xiao, Jiachen Shang, Xiao Xu, Luo He and Yu Xiang,*

Department of Chemistry, Key Laboratory of Bioorganic Phosphorus Chemistry and Chemical Biology (Ministry of Education), Beijing Key Laboratory for Microanalytical Methods and Instrumentation, Tsinghua University, Beijing 100084, China

*Email: xiang-yu@tsinghua.edu.cn

Table S1. List of the target sequences in EMX1 and HBB, the two off-target sequences used as the DNA substrates, and the primers used for their PCR amplifications in this study.

Name	Sequence (left to right: 5′ to 3′)	Chr Position
EMX1 target sequence	GAGTCCGAGCAGAAGAAGAA	Chr2:72933853-72933875
EMX1 fw	AAAACCACCCTTCTCTCTGGC	
EMX1 rv	GGAGATTGGAGACACGGAGAG	
EMX1 OT1 sequence	GAGTTAGAGCAGAAGAAGAA	Chr5:45358959-45358981
EMX1 OT1 fw	GACACCTTTTAAGATCTGACAGAGAAACATTTACC	
EMX1 OT1 rv	CACAAACTGGTAATAGATTAACAGGAAAAAAGGGC	
EMX1 OT2 sequence	AGTCAGAGGAGAAGAAGAA	Chr15:61354663-61354684
EMX1 OT2 fw	GGTCCAGATAGTATTGAGGCCAAC	
EMX1 OT2 rv	CAGTAGTTAATGTCCAGCCCAGAG	
HBB target sequence	CTTGCCCCACAGGGCAGTAA	Chr11:5226968-5226990
HBB fw	CCAACTCCTAAGCCAGTGCCAGAAGAG	
HBB rv	ACTCAGTGCCTATCAGAAACCCAAGAG	

Note: The “fw” and “rv*” represent forward and reverse primers, respectively. “OT” is off-target. Underlined are the different oligonucleotides in the OT sequences compared with the target sequence.

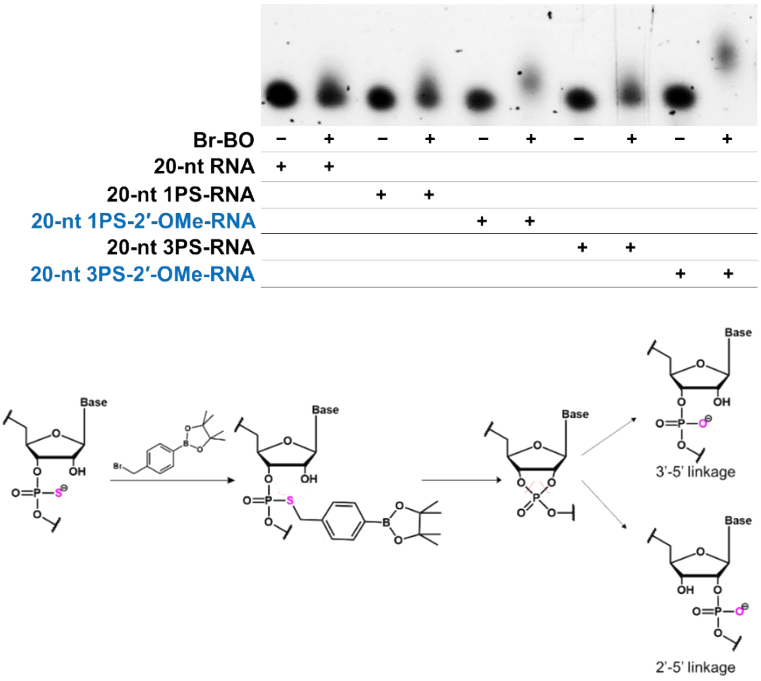

Figure S1. BO modification was successfully incorporated in RNA PS-2′-OMe but failed in RNA PS-2′-OH. The reaction between PS-2′-OH and BO-Br possibly yielded a cyclic phosphotriester, which could undergo hydrolysis and should give 3′-5′ and 2′-5′ RNA linkages as two major products.

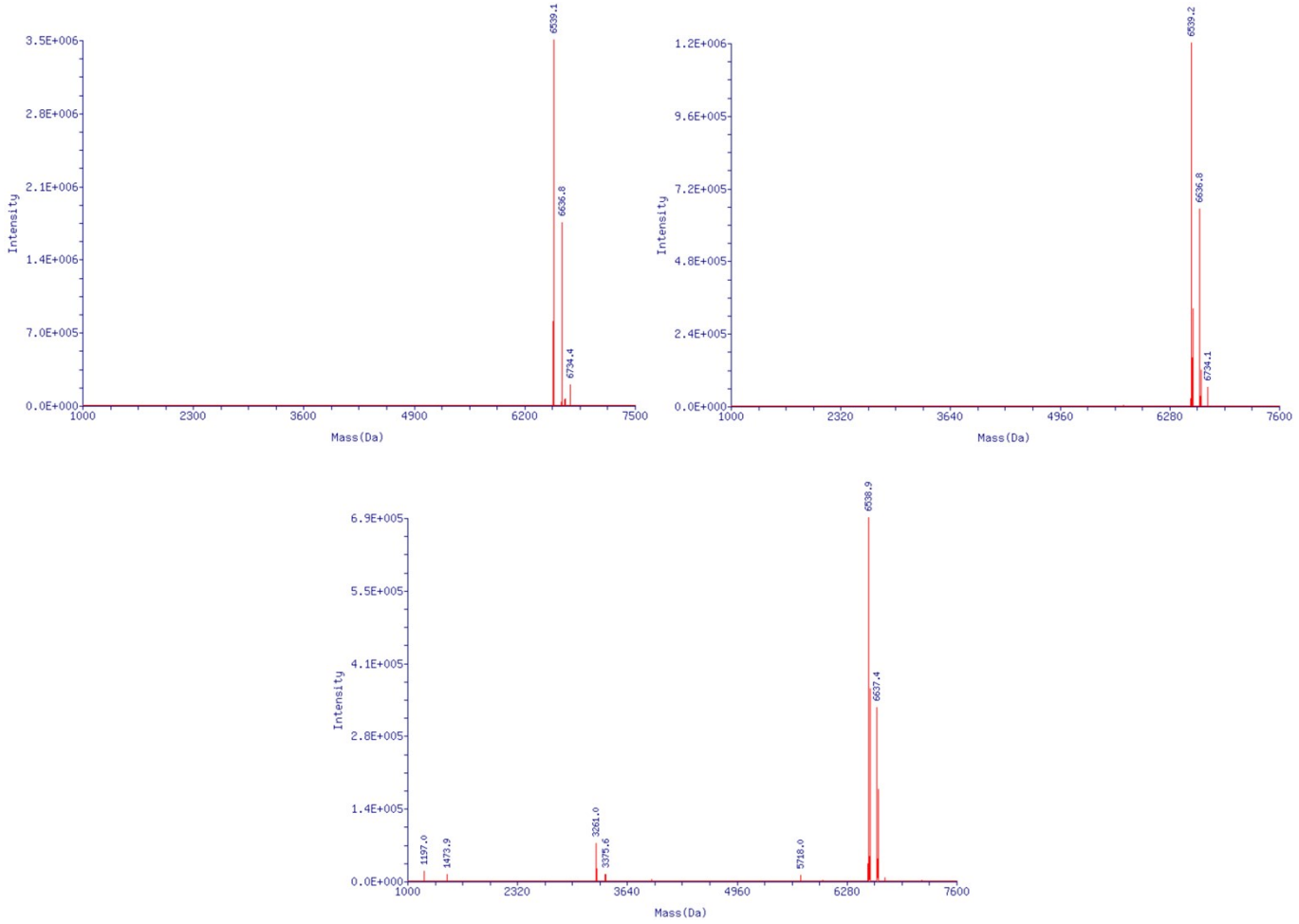

Figure S2. No attachment of BO to native RNA oligonucleotides or those with PS-2′-OH was found after reaction with BO-Br. For each PS-2′-OH in RNA, the BO-Br reaction leads to the formation of 3′-5′ and 2′-5′ RNA linkages without phosphorothioate (S-to-O change, mass −16). *Top left:* ESI-MS of 20-nt RNA after reaction with BO-Br: calc. 6539.1 (M, 20-nt RNA); found 6539.1 (M), 6636.8 (M+H_3PO_4). *Top right:* ESI-MS of 20-nt 1PS-RNA after reaction with BO-Br: calc. 6555.1 (M, 20-nt 1PS-RNA); found 6539.2 (M−16), 6636.8 (M−16+H_3PO_4). *Bottom:* ESI-MS of 20-nt 3PS-RNA after reaction with BO-Br: calc. 6587.1 (M, 20-nt 3PS-RNA); found 6538.9 (M−3*16), 6637.4 (M−3*16+H_3PO_4). The second strongest peak in each spectrum is adduct with one phosphate (+98, H_3PO_4), occasionally observed due to the mass spectrum analysis using samples in a diluted phosphate buffer.

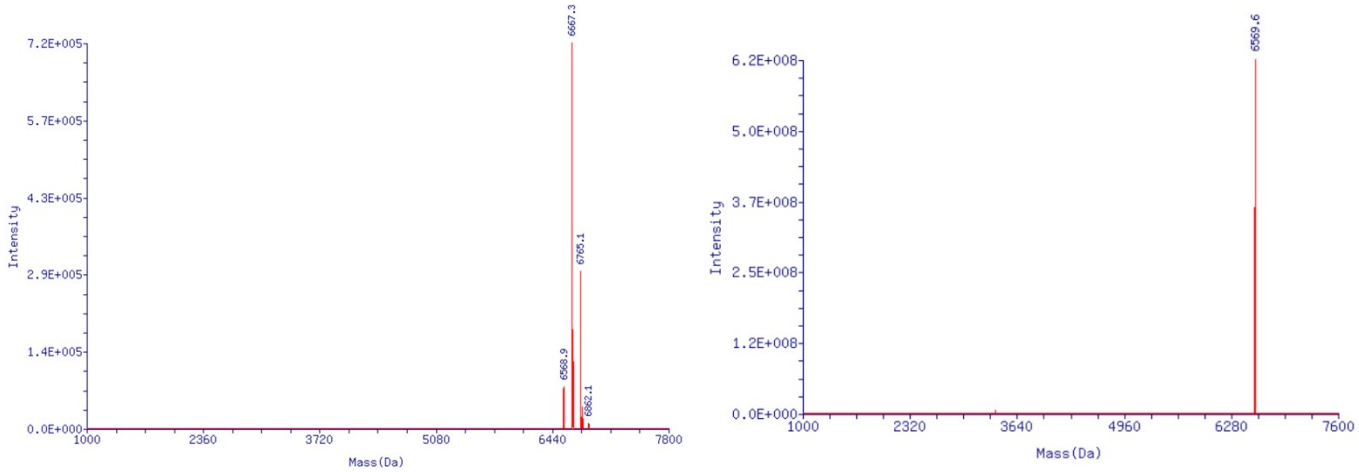

Figure S3a. *Left:* ESI-MS of 20-nt 1BO-RNA: calc. 6785.3 (M); found 6667.3 (M−pinacol). *Right:* ESI-MS of 20-nt 1BO-RNA after H_2O_2 treatment to remove BO: calc. 6569.6 (20-nt 1PS-2′-OMe-RNA); found 6569.5. We thought the loss of pinacol from 1BO-RNA in the mass spectrum was more likely caused by the ionization process of ESI-MS measurement rather than the hydrolysis of pinacol ester in the buffers, because many phenylboronic acid pinacol ester-based sensors were reported stable for intracellular sensing of H_2O_2 (Srikun, D.; Miller, E. W.; Dornaille, D. W.; Chang, C. J. *J. Am. Chem. Soc.* **2008**, *130*, 4596. Saravanakumar, G.; Kim, J.; Kim, W. J. *Adv. Sci.* **2017**, *4*, 1600124.). Related to Figure 1B.

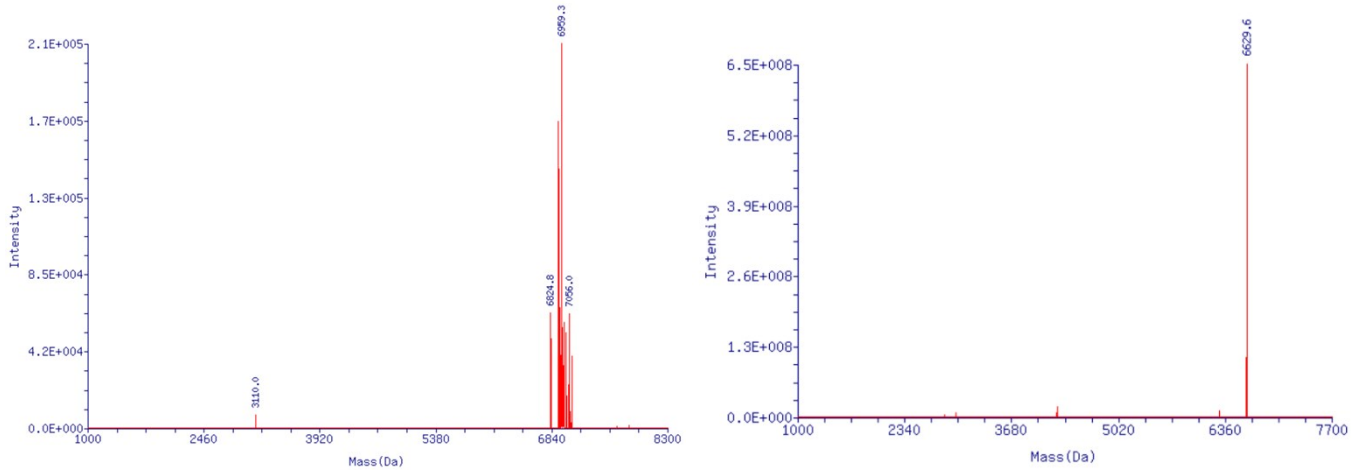

Figure S3b. *Left:* ESI-MS of 20-nt 3BO-RNA: calc. 7277.9 (M); found 6959.3 (M−3*pinacol+2*H_2O). *Right:* ESI-MS of 20-nt 3BO-RNA after H_2O_2 treatment to remove BO: calc. 6629.3 (3PS-2′-OMe-RNA); found 6629.6. Related to Figure 1B.

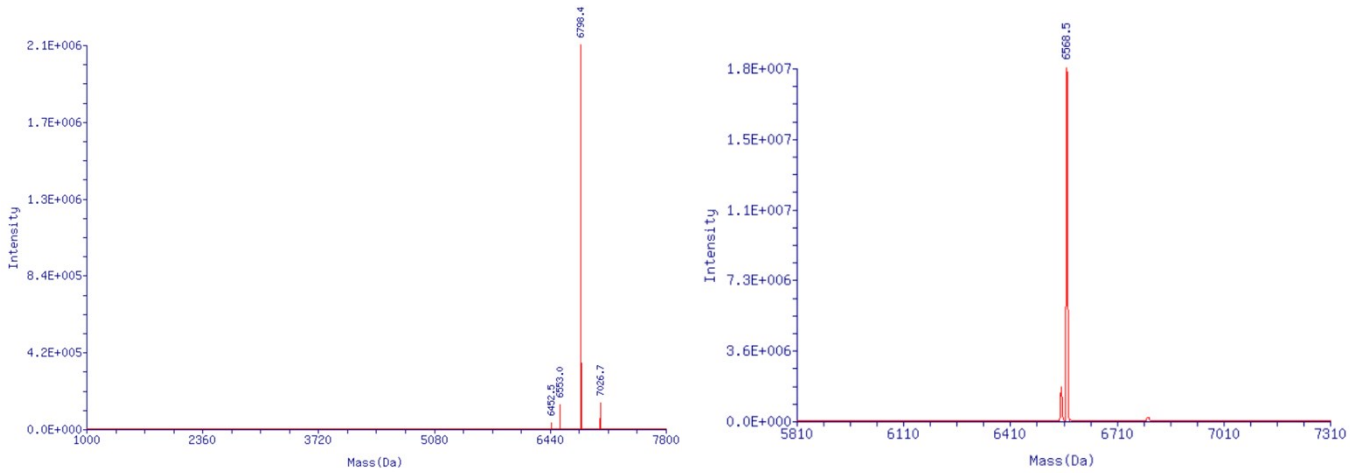

Figure S3c. *Left:* ESI-MS of 20-nt 1CM-RNA: calc. 6798.2 (M); found 6798.4. *Right:* ESI-MS of 20-nt 1CM-RNA after visible light irradiation to remove CM: calc. 6569.1 (20-nt 1PS-2′-OMe-RNA); found 6568.5. Related to Figure 1E.

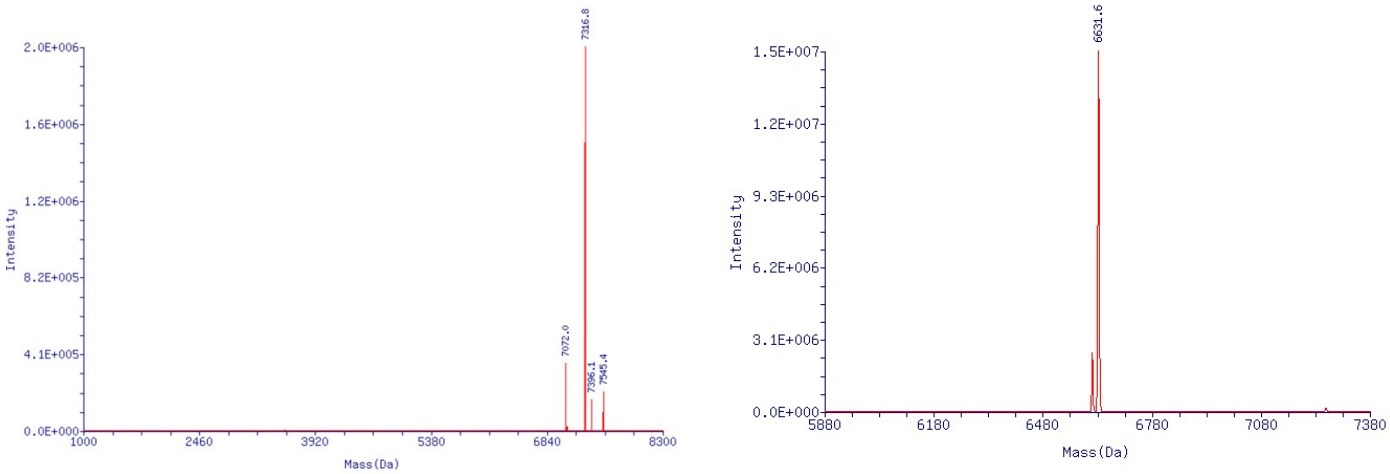

Figure S3d. *Left:* ESI-MS of 20-nt 3CM-RNA: calc. 7316.5 (M); found 7316.8. *Right:* ESI-MS of 20-nt 3CM-RNA after visible light irradiation to remove CM: calc. 6629.1 (20-nt 3PS-2′-OMe-RNA); found 6631.6. Related to Figure 1E.

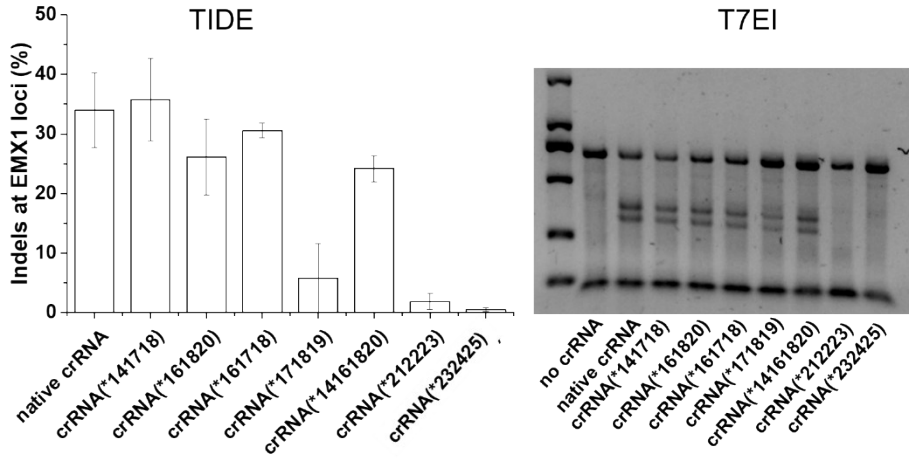

Figure S4. Screening the genome editing activities of PS-2′-OMe-RNA$_{EMX1}$ designs in HEK 293T-Cas9 cells using TIDE and T7E1 assays, transfected along with tracrRNA.

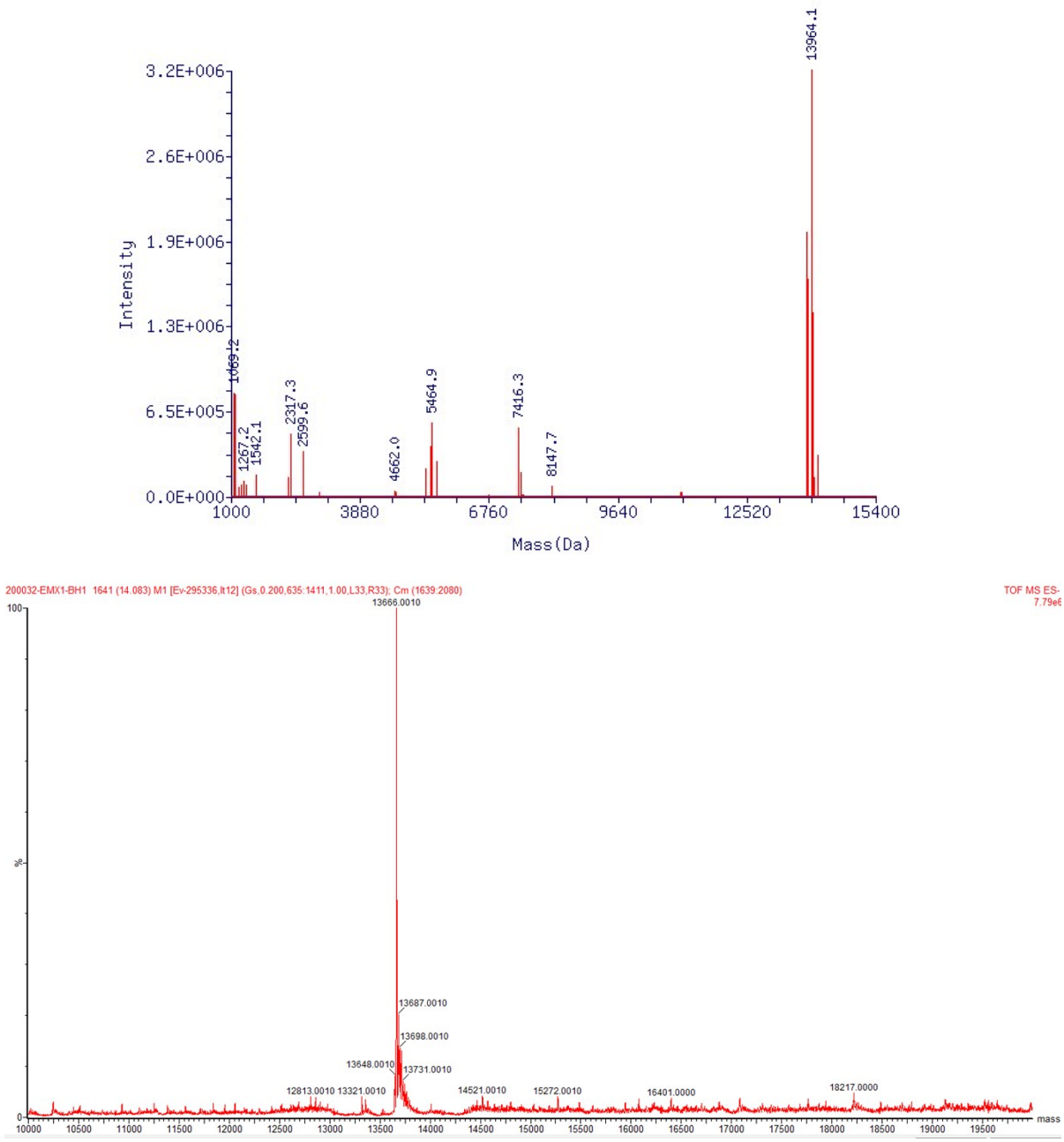

Figure S5a. ESI-MS of 3BO-141718-crRNA$_{EMX1}$ before (*Top:* calc. 14314.9 (M), found 13964.1 (M−3*pinacol) and after (*Bottom:* calc. 13666.6 (PS-2′-OMe-141718-crRNA$_{EMX1}$), found 13666.0) reacting with 1 mM H_2O_2 for 1 h at 37 °C. Related to Figure 2B.

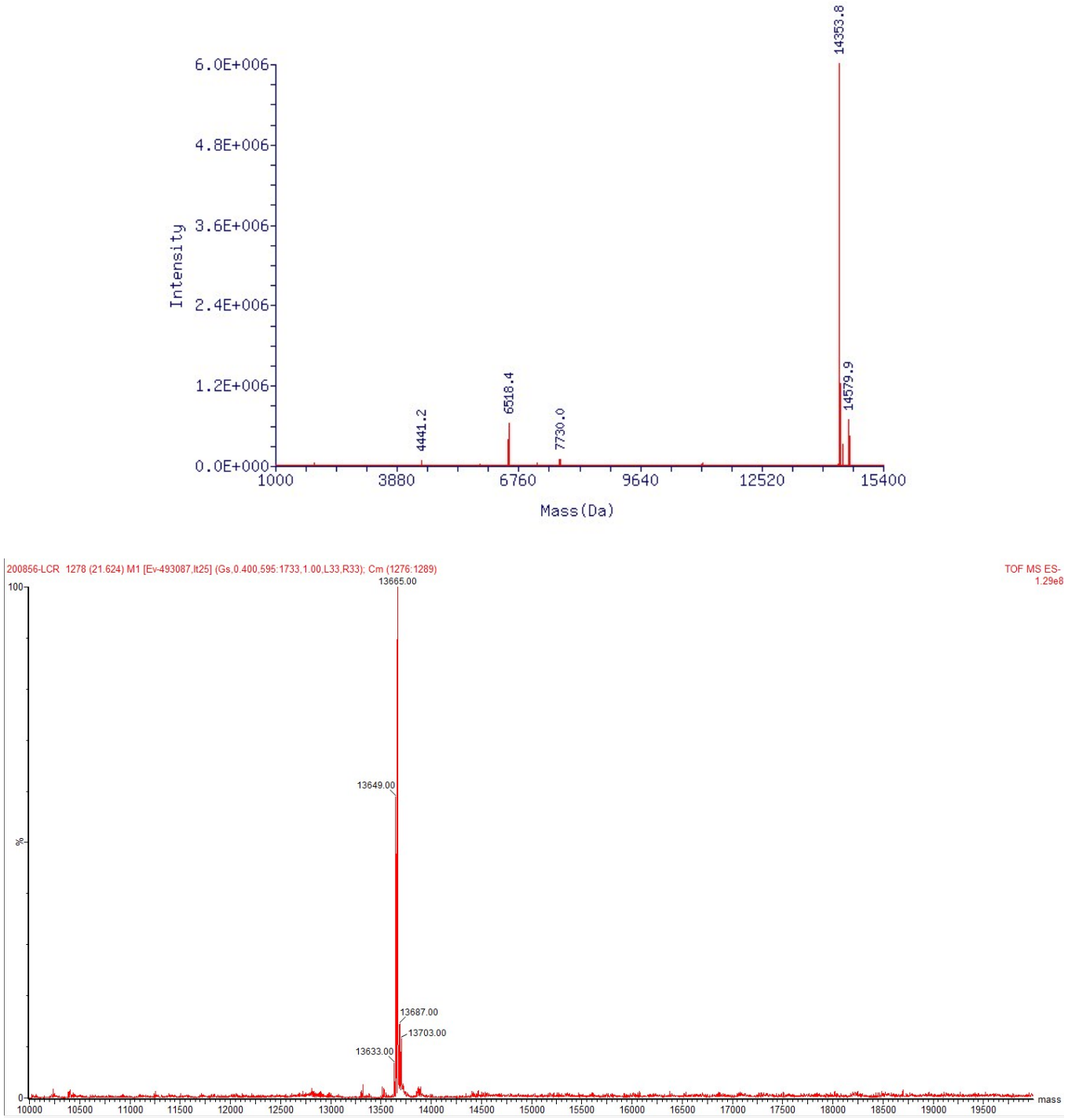

Figure S5b. ESI-MS of 3CM-141718-crRNA$_{EMX1}$ before (*Top:* calc. 14353.0 (M), found 14353.8) and after (*Bottom:* calc. 13666.6 (PS-2′-OMe-141718-crRNA$_{EMX1}$), found 13665.0) visible light (470 nm) irradiation at 13 mW/cm^2 for 30 min at 37 ^{o}C. Related to Figure 2D.

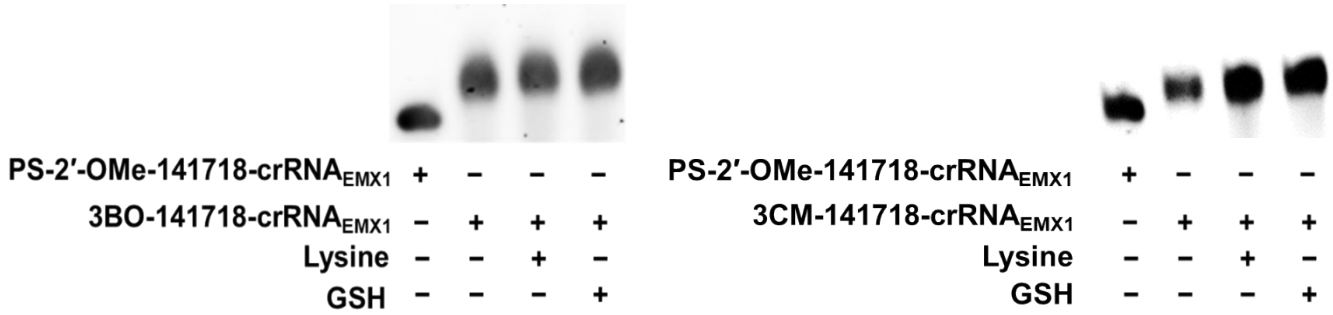

Figure S6. Stability of 3BO-141718-crRNA$_{EMX1}$ (*Left*) and 3CM-141718-crRNA$_{EMX1}$ (*Right*) in the presence of 5 mM lysine or 5 mM GSH for 4 h in 1xNEBuffer™ 3.1 buffer at 37 °C.

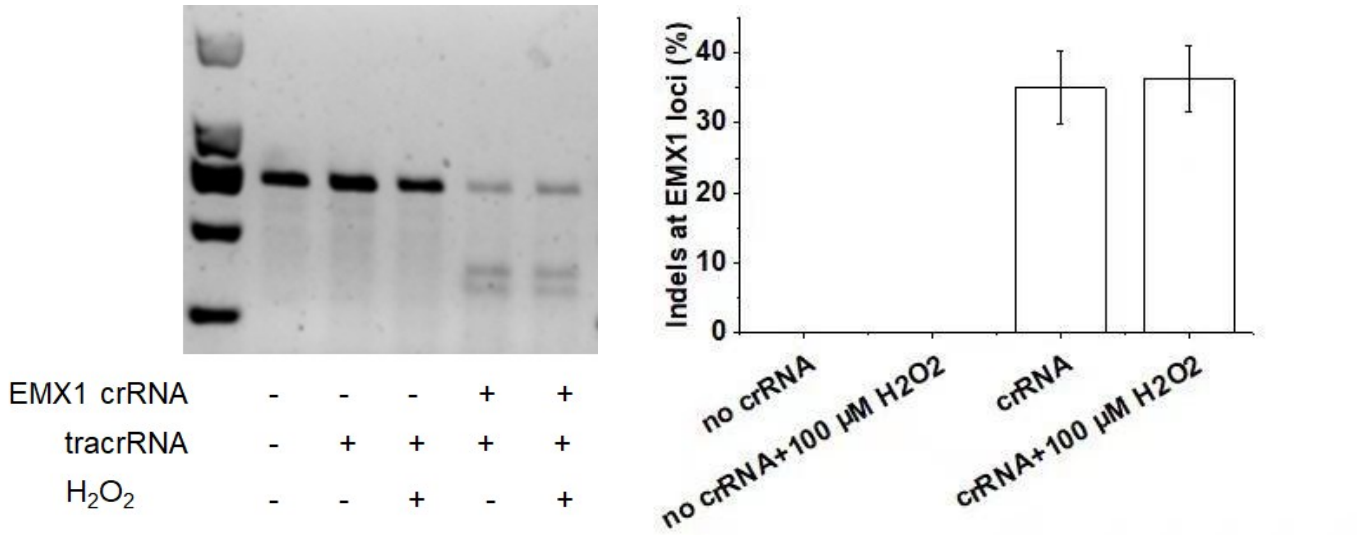

Figures S7. T7E1 (*Left*) and TIDE (*Right*) assays of editing efficiency of Cas9 and tracrRNA in the absence and presence of crRNA$_{EMX1}$ in cells under oxidative stress or not, to show that oxidative stress itself induces neither background indels in the absence of crRNA nor additional editing in the presence of crRNA.

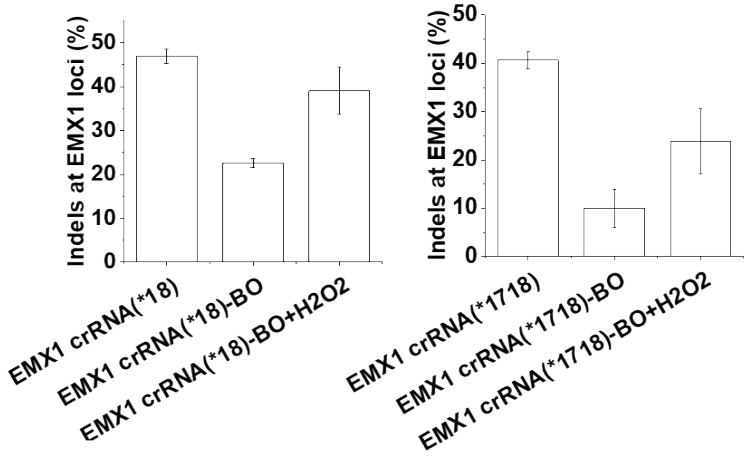

Figure S8a. TIDE assays of editing efficiency of BO-18-crRNA$_{EMX1}$ (*Left*) and 2BO-1718-crRNA$_{EMX1}$ (*Right*) in normal 293T-Cas9 cells and in 293T-Cas9 cells under oxidative stress (labeled with +H_2O_2), transfected along with tracrRNA. These cellular studies used the same procedures as the TIDE experiment for 3BO-141718-crRNA$_{EMX1}$.

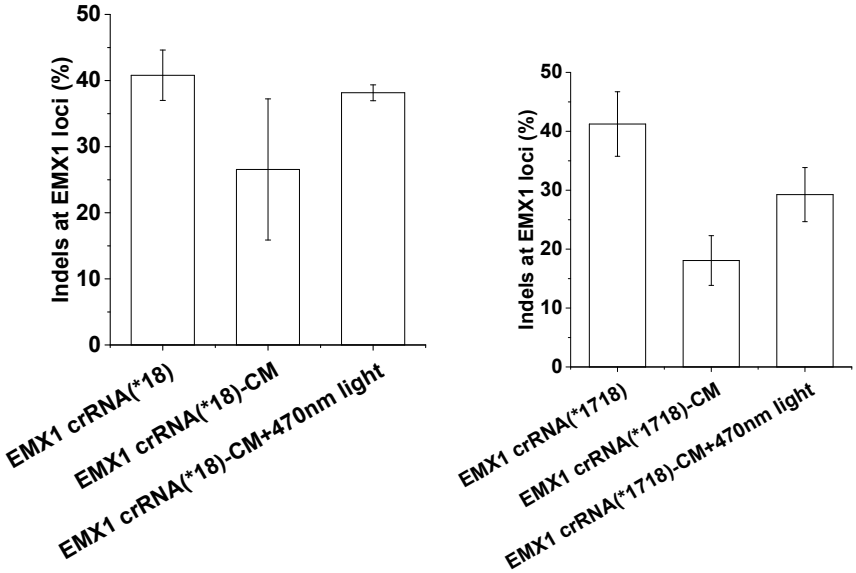

Figure S8b. TIDE assays of editing efficiency of CM-18-crRNA$_{EMX1}$ (*Left*) and 2CM-1718-crRNA$_{EMX1}$ (*Right*) in 293T-Cas9 cells with and without visible light irradiation, transfected along with tracrRNA. These cellular studies used the same procedures as the TIDE experiment for 3CM-141718-crRNA$_{EMX1}$.

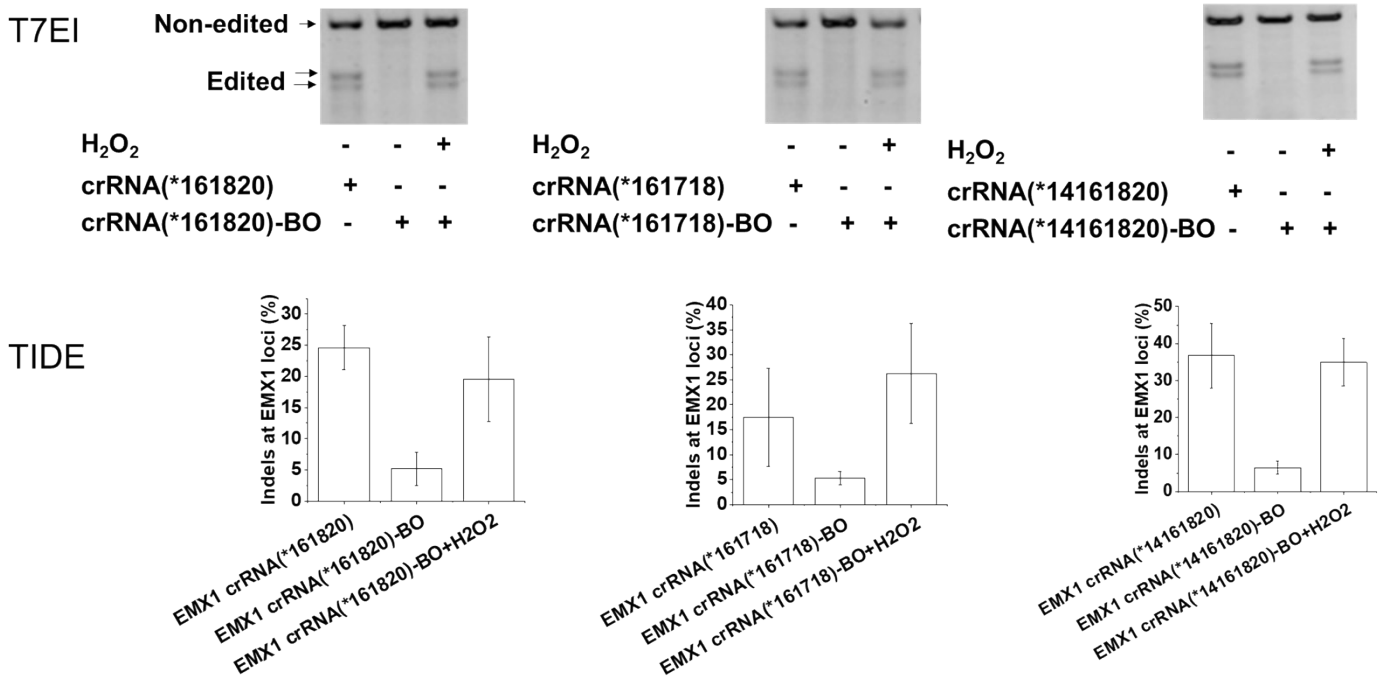

Figure S9. T7E1 and TIDE assays of editing efficiency of 3BO-161820-crRNA$_{EMX1}$ (left), 3BO-161718-crRNA$_{EMX1}$ (middle) and 4BO-14161820-crRNA$_{EMX1}$ (right) in normal 293T-Cas9 cells and in 293T-Cas9 cells under oxidative stress (labeled with +H_2O_2), transfected along with tracrRNA. These cellular studies used the same procedures as the TIDE experiment for 3BO-141718-crRNA$_{EMX1}$.

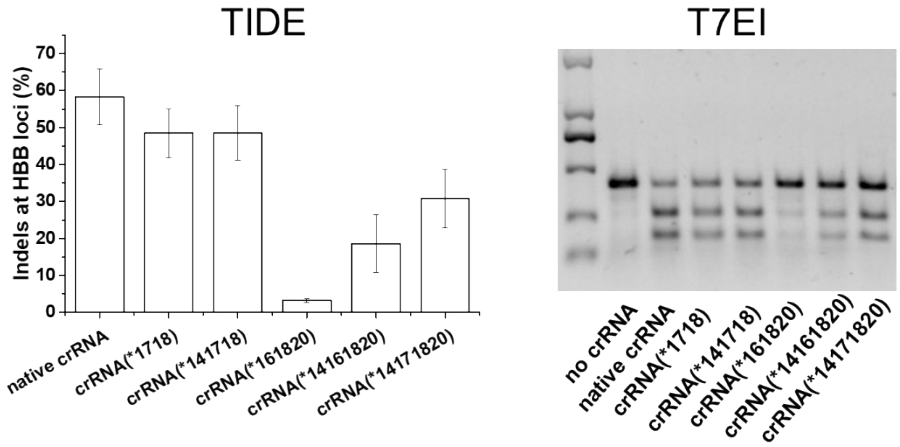

Figure S10. Screening the gene-editing activities of PS-2′-OMe-modified crRNA$_{HBB}$ designs in 293T cells using TIDE and T7E1 assays, transfected along with tracrRNA and Cas9 mRNA.

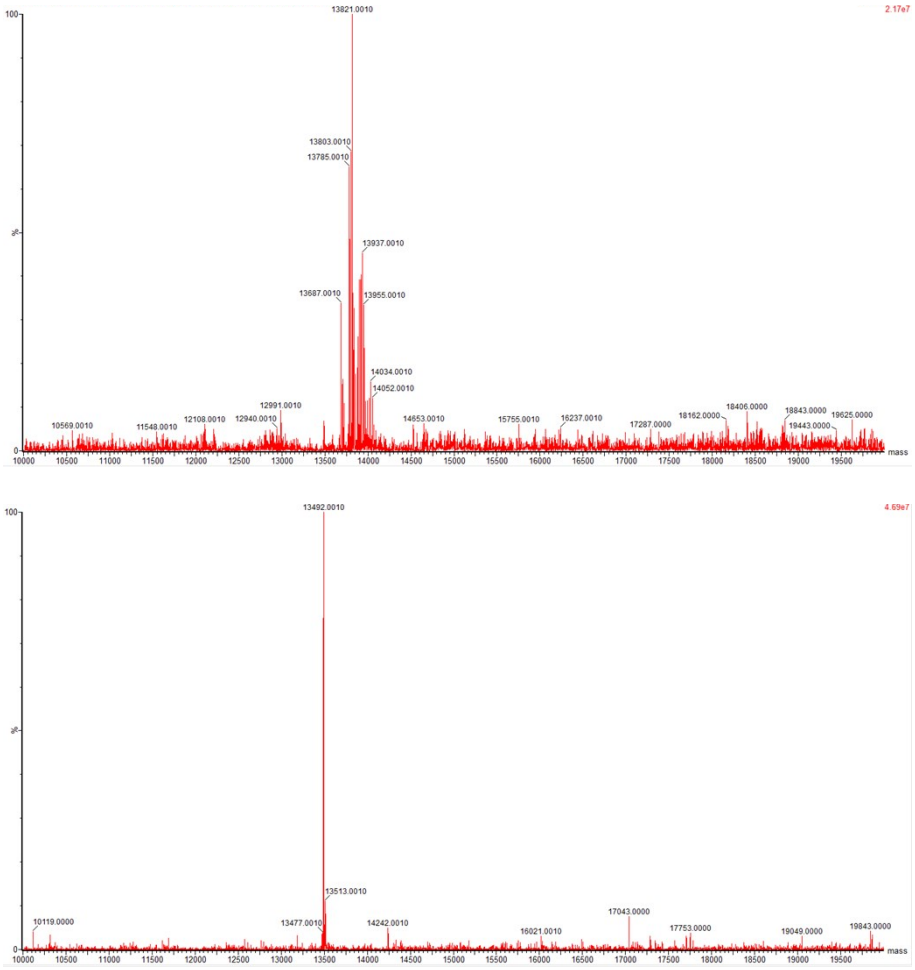

Figure S11. ESI-MS of 3BO-141718-crRNA$_{HBB}$ before (*Top:* calc. 14140.8 (M), found 13821.0 (M−3*pinacol+2*H_2O), 13937.0 (M−2*pinacol+2*H_2O)) and after (*Bottom:* calc. 13492.2 (PS-2′-OMe-141718-crRNA$_{HBB}$), found 13492.0) reacting with 1 mM H_2O_2 for 1 h at 37 °C. Related to Figure 4.

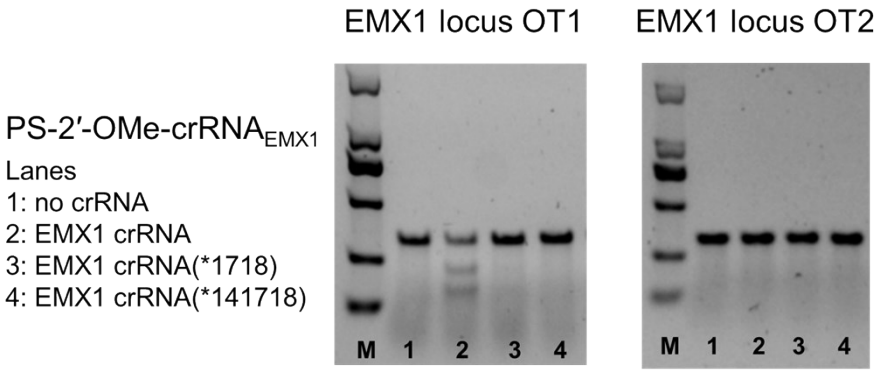

Figure S12. T7E1 assays of editing efficiency of crRNA$_{EMX1}$ (lane 2), 2PS-2′-OMe-1718-crRNA$_{EMX1}$ (lane 3) and 3PS-2′-OMe-141718-crRNA$_{EMX}$ (lane 4) in 293T-Cas9 cells, transfected along with tracrRNA, respectively. Lane 1 is the negative control without crRNA. The results suggested that both of the two PS-2′-OMe-modified crRNAs were at least as selective as the native crRNA on the EMX1 target site over the two off-target sides OT1 and OT2. See Table S1 for the sequences of OT1/OT2 and primers used for the preparation of DNA samples in the T7E1 assays.

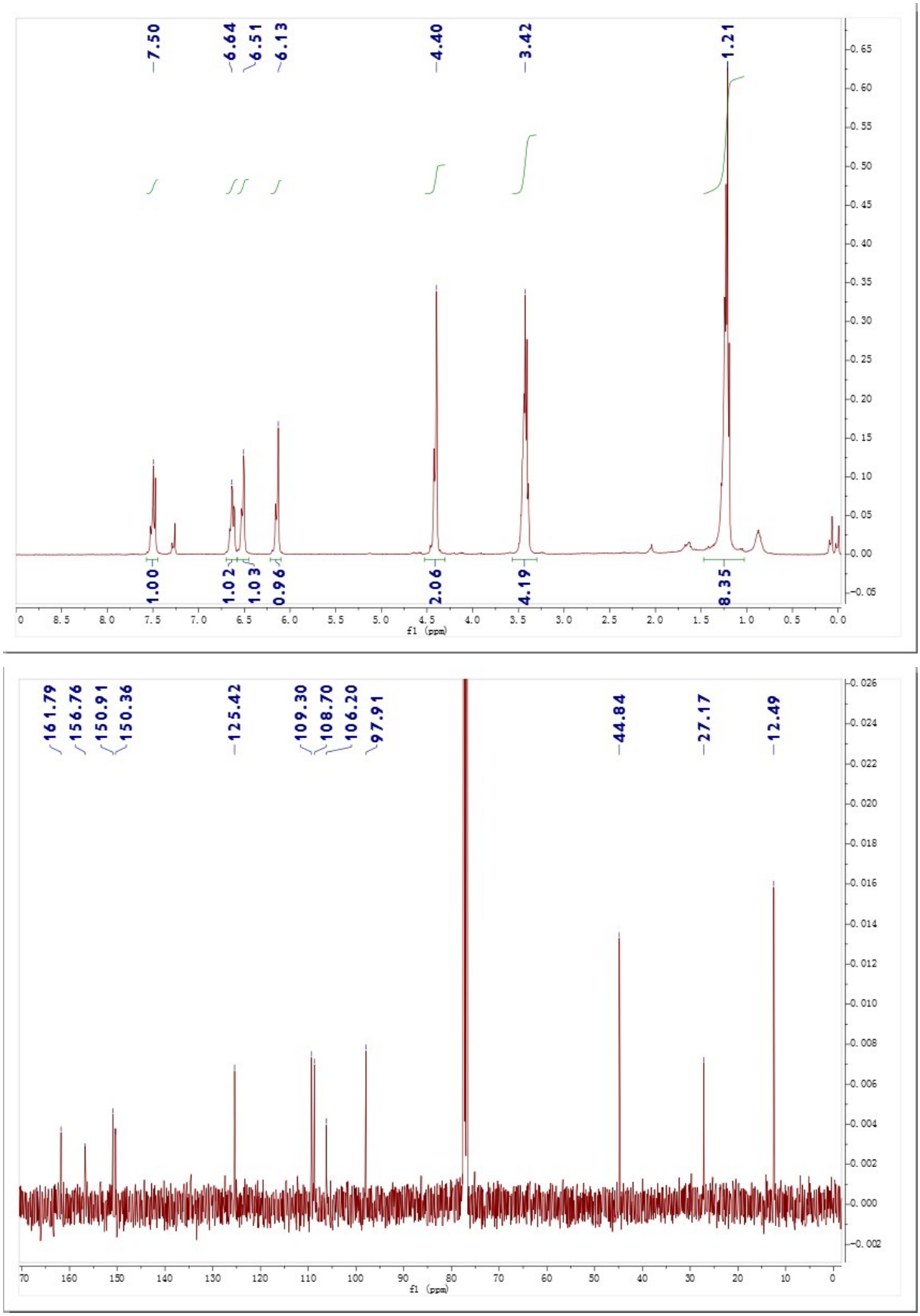

Figure S13. ^{1}H-NMR and ^{13}C-NMR spectra (300 MHz) of CM-Br in $CDCl_3$.